Journal of Sound and Vibration (2001) **240**(3), 447–465
doi:10.1006/jsvi.2000.3236, available online at http://www.idealibrary.com on IDEAL®

IMPACT STUDY OF CABLE-STAYED BRIDGE UNDER RAILWAY TRAFFIC USING VARIOUS MODELS

F. T. K. Au

Department of Civil Engineering, The University of Hong Kong, Pokfulam Road, Hong Kong, People's Republic of China. E-mail: hrecatk@hku.hk

J. J. Wang

Department of Civil Engineering, Hunan University, Yuelushan, Changsha, Hunan 410082, *People's Republic of China*

AND

Y. K. Cheung

Department of Civil Engineering, The University of Hong Kong, Pokfulam Road, Hong Kong, People's Republic of China

(*Received* 18 *January* 2000, *and in final form* 15 *June* 2000)

In routine bridge designs, the dynamic effects of the moving vehicles on bridges are taken into account by increasing the static loads by an impact factor. This impact factor depends on many things, and various design codes indeed give different guidance on the impact factor. This paper describes a study on the impact effects on a cable-stayed bridge under railway train loading. The cable-stayed bridge is modelled as a planar system. The rail irregularities and the geometric non-linear behaviour of the cable-stayed bridge are taken into account. The train comprises a number of cars, and numerical models of various degrees of sophistication are investigated. They include the sophisticated model comprising a 4-axle system possessing 10 degrees of freedom (d.o.f.), and the simplified models comprising a series of 2-d.o.f. mass–spring–damper systems, moving masses or moving forces. The impact factors for various speeds are evaluated using a typical cable-stayed bridge with various models for the train. The models are then reviewed in the light of such results.

1. INTRODUCTION

Cable-stayed bridges have been extensively employed in the construction of major crossings over the last three decades because of their aesthetic appeal, structural efficiency, ease of construction, small size of substructures and enhanced stiffness compared with suspension bridges. With the rapid increase in span length, combined with the trend to use lighter and high-strength materials and therefore more slender sections for the bridge deck, concern has been raised on the dynamic behaviour of cable-stayed bridges, especially under increasingly heavy and fast moving loads.

In the dynamic analysis of such combined systems, the engineer has to decide a suitable model for the moving vehicles as well as how the fast moving heavy vehicles interact with the bridge structure. Theoretically, a moving load model may be used where the inertia of the vehicle is small compared to that of the bridge and the method has been adopted by

0022-460X/01/080447 + 19 $35.00/0

various researchers [1–6]. Where the inertia of the vehicle cannot be taken as small, the mass has to be somehow accounted for. A moving vehicle can be modelled as a one-foot dynamic system having two degrees of freedom (d.o.f.) [7–9]. More realistic multi-axle vehicles have also been employed in the dynamic analysis of various types of highway bridge [10–13]. Similarly, in the dynamic analysis of railway bridges, the train has been modelled as a series of moving loads or axles [9, 14]. Some other researchers have adopted more sophisticated multi-axle models for the train cars [15–17].

There are two methods to account for the interaction between the moving vehicles and the bridge structures. In the first approach, coupled equations of motion are formulated for the entire bridge–vehicle system and these equations are subsequently solved by direct time integration such as the Newmark or Wilson-θ method. This method was used by most researchers [9, 15, 17]. In the other approach, two uncoupled sets of equations are set up for the bridge and the vehicles respectively. The two sets of equations are then solved in an iterative manner to ensure the geometrical compatibility and force equilibrium conditions at the vehicle–bridge interface [10–12].

The use of sophisticated train models to study the dynamic response of cable-stayed bridges appears rare. The investigation by Huang and Wang [18] of dynamic response of cable-stayed bridges was to certain extent similar but the load was a single 3-axle 7-d.o.f. moving truck instead of a train. Wiriyachai *et al.* [15] used a 4-axle train model to study the impact effects on simply supported truss bridges. Yang and Fonder [5] employed a moving load model to investigate the dynamic response of a cable-stayed bridge having a main span of 150 m. Yang *et al.* [17] adopted a 6-axle vehicle model in the dynamic analysis of a cable-stayed bridge with a 60 m main span.

This paper describes a study on the impact effects on a cable-stayed bridge under railway train loading. The cable-stayed bridge is modelled as a planar system, which is good enough for the study of impact effects under the railway traffic although it is unable to predict the behaviour associated with the torsional modes. Non-linear static analysis of the bridge is first performed to get the internal forces in the bridge deck, towers and stay cables under the permanent loading. Non-linearities such as those arising from the sag of stay cables, beam–column behaviour of the bridge deck and towers, and geometrical large displacements are taken into account in the static analysis.

The internal forces obtained from the static analysis are then utilized to build up the model which is necessary for the dynamic analysis. The rail irregularities and the geometric non-linear behaviour of the cable-stayed bridge are taken into account. The train comprises a number of cars, which are modelled using various methods. They include the sophisticated model comprising a 4-axle system possessing 10 d.o.f., and the simplified models comprising a series of 2-d.o.f. mass–spring–damper systems, moving masses or moving forces. The impact effects for various speeds are then evaluated using a typical cable-stayed bridge. The various models employed are then reviewed in the light of such results.

2. THE TRAIN MODEL

A typical railway vehicle consists of the vehicle body carrying passengers or freight and the wheels. The body is supported either directly on their axles or on bogies. The increasingly heavy loading has called for more axles grouped into bogies, where two or more axles are mounted on the same frame. The bogie frames are connected to the axles and to the railway vehicle body, respectively, through the primary and secondary suspension systems, which comprise springs and shock absorbers.

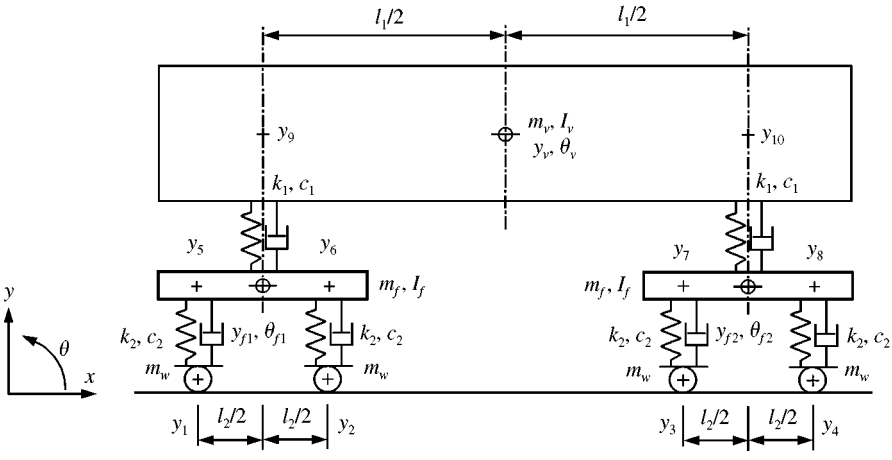

Figure 1. Model of a typical train vehicle for the analysis of vehicle–bridge interaction.

Figure 1 shows the train vehicle model adopted in the present study. The vehicle body is modelled as a rigid body having a mass m_v and a moment of inertia I_v about the transverse horizontal axis through its centroid. Similarly, each bogie frame is considered as a rigid body with a mass m_f and a moment of inertia I_f about the transverse horizontal axis through its centroid. Each axle along with the wheels has a mass m_w. The spring and shock absorber in the primary suspension for each axle are characterized by spring stiffness k_2 and damping coefficient c_2 respectively. Likewise the secondary suspension is characterized by spring stiffness k_1 and damping coefficient c_1. The vertical displacements of the train vehicle model are described by y_1 to y_{10} at locations marked by crosses in Figure 1 with respect to their equilibrium positions before coming to the bridge. As the vehicle body is assumed to be rigid, its motion may be described by the vertical displacement y_v and rotation θ_v at its centroid instead of y_9 and y_{10}. Similarly, the vertical motions of the bogie frames may also be described by y_{f1}, θ_{f1}, y_{f2} and θ_{f2} at their centroids instead of y_5 to y_8. The displacement vector δ_t for the train vehicle can therefore be written in terms of displacements at the centroid of the vehicle body y_v and θ_v, the displacements at the centroids of the bogie frames y_{f1}, θ_{f1} y_{f2} and θ_{f2}, and the displacements of the four axles y_1 to y_4 as

$$\delta_t = [y_v \;\; \theta_v \;\; y_{f1} \;\; \theta_{f1} \;\; y_{f2} \;\; \theta_{f2} \;\; y_1 \;\; y_2 \;\; y_3 \;\; y_4]^{\mathrm{T}}. \tag{1}$$

Figure 2 shows the same train vehicle model with the vehicle body, the bogie frames and the axles isolated as free bodies. The internal forces and inertia forces are also shown. The reactions at the rail, and at the primary and secondary suspension systems are expressed in terms of the static reaction components R_w, R_p and R_s, respectively, as well as the dynamic reaction components f_{c1} to f_{c4} and f_1 to f_6. The static reaction components R_w, R_p and R_s are given as

$$R_w = m_v g/4 + m_f g/2 + m_w g, \tag{2}$$

$$R_p = m_v g/4 + m_f g/2, \tag{3}$$

$$R_s = m_v g/4, \tag{4}$$

where g is the acceleration due to gravity. The equations of motion of each free body can then be formulated, and they are given in Appendix A. As the static case is one particular

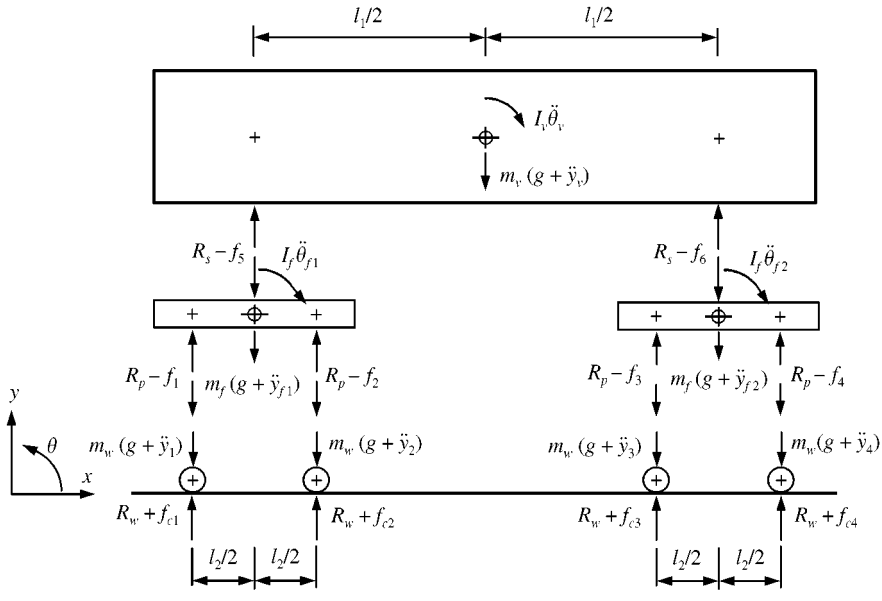

Figure 2. Internal forces acting in the 4-axle model of typical train vehicle.

case of the dynamic situation, the static reaction components cancel themselves and do not appear in these equations. The equation of motion can be written in matrix notation in terms of the mass matrix $\mathbf{m}_t$, the damping matrix $\mathbf{c}_t$, the stiffness matrix $\mathbf{k}_t$ and the load vector $\mathbf{f}_t$ for the train vehicle as

$$\mathbf{m}_t\ddot{\delta}_t + \mathbf{c}_t\dot{\delta}_t + \mathbf{k}_t\delta_t = f_t, \tag{5}$$

where the dot denotes differentiation with respect to time t. The displacement vector δ_t for the train vehicle can be divided into the upper group δ_u^t, which are unconstrained by the bridge, and the lower group δ_{I}^t, which are in contact with the bridge, where

$$\delta_u^t = [y_v \;\; \theta_v \;\; y_{f1} \;\; \theta_{f1} \;\; y_{f2} \;\; \theta_{f2}]^{\mathrm{T}}, \tag{6}$$

$$\delta_{\mathrm{I}}^t = [y_1 \;\; y_2 \;\; y_3 \;\; y_4]^{\mathrm{T}}. \tag{7}$$

The equation of motion for the train model can be written in terms of the sub-matrices and sub-vectors as

$$\begin{bmatrix} \mathbf{m}_{uu}^t & \\ & \mathbf{m}_{\mathrm{II}}^t \end{bmatrix} \begin{Bmatrix} \ddot{\delta}_u^t \\ \ddot{\delta}_{\mathrm{I}}^t \end{Bmatrix} + \begin{bmatrix} \mathbf{c}_{uu}^t & \mathbf{c}_{u\mathrm{I}}^t \\ \mathbf{c}_{\mathrm{I}u}^t & \mathbf{c}_{\mathrm{II}}^t \end{bmatrix} \begin{Bmatrix} \dot{\delta}_u^t \\ \dot{\delta}_{\mathrm{I}}^t \end{Bmatrix} + \begin{bmatrix} \mathbf{k}_{uu}^t & \mathbf{k}_{u\mathrm{I}}^t \\ \mathbf{k}_{\mathrm{I}u}^t & \mathbf{k}_{\mathrm{II}}^t \end{bmatrix} \begin{Bmatrix} \delta_u^t \\ \delta_{\mathrm{I}}^t \end{Bmatrix} + \begin{Bmatrix} \mathbf{f}_u^t \\ \mathbf{f}_{\mathrm{I}}^t \end{Bmatrix}, \tag{8}$$

where the sub-matrices and sub-vectors are given in Appendix A. Notice that the load sub-vector $\mathbf{f}_u^t$ is zero. The load sub-vector $\mathbf{f}_{\mathrm{I}}^t$ comprises the transient components only as the displacements in the sub-vector δ_u^t of the train are given with respect to their equilibrium positions before coming to the bridge. Therefore, the total reactions $\bar{\mathbf{f}}_{\mathrm{I}}^t$ between the train axles and the bridge have to include the static reactions also, i.e.,

$$\bar{\mathbf{f}}_{\mathrm{I}}^t = \mathbf{R}_w + \mathbf{f}_{\mathrm{I}}^t = [R_w \;\; R_w \;\; R_w \;\; R_w]^{\mathrm{T}} + [f_{c1} \;\; f_{c2} \;\; f_{c3} \;\; f_{c4}]^{\mathrm{T}}. \tag{9}$$

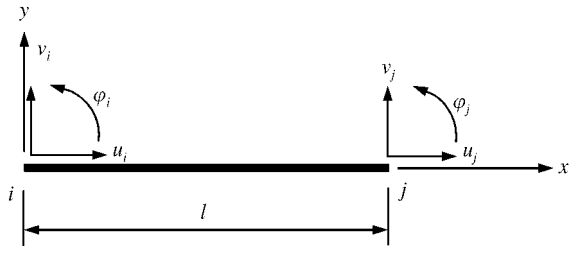

Figure 3. Degrees of freedom of a typical beam element.

3. THE BRIDGE MODEL

The cable-stayed bridge is modelled as a planar system. Beam elements are used to model the bridge deck and towers. The deformation of each beam element is defined by the d.o.f. at the end nodes i and j. The displacement vector δ_b^e of the beam element therefore appears as

$$\delta_b^e = [u_i \;\; v_i \;\; \varphi_i \;\; u_j \;\; v_j \;\; \varphi_j]^{\mathrm{T}}, \tag{10}$$

where u and v are the translational displacements along the local x- and y-axes, respectively, and φ is the rotational displacement, as shown in Figure 3. The stiffness matrix $\mathbf{k}_b^e$ of the beam element subjected to an axial force can be written in terms of the linear stiffness matrix $\mathbf{k}_{b\mathrm{I}}^e$ and the geometric stiffness matrix $\mathbf{k}_{bg}^e$ as

$$\mathbf{k}_b^e = \mathbf{k}_{b\mathrm{I}}^e + \mathbf{k}_{bg}^e. \tag{11}$$

The stay cables are modelled as single-bar elements and the non-linear catenary effect is taken into account using the equivalent modulus of elasticity E_{eq} given by

$$E_{eq} = \frac{E_c}{1 + (wH)^2 A_c E_c / 12T^3}, \tag{12}$$

where H is the horizontal projected length of the cable, A_c is the cross-sectional area, E_c is the effective material modulus of elasticity of stay cable, w is the weight per unit length of the cable and T is the prevailing cable tension obtained for permanent loading.

After the standard procedures of formation and transformation of the element matrices and vectors, followed by the standard assembly process, the equation of motion for the bridge can therefore be written as

$$\mathbf{m}_b \ddot{\delta}_b + \mathbf{c}_b \dot{\delta}_b + \mathbf{k}_b \delta_b = -\mathbf{N}_b^{\mathrm{T}} \bar{\mathbf{f}}_{\mathrm{I}}^t \tag{13}$$

in terms of the mass matrix $\mathbf{m}_b$, the damping matrix $\mathbf{c}_b$, the stiffness matrix $\mathbf{k}_b$ and the displacement vector δ_b for the entire bridge, the shape function matrix $\mathbf{N}_b$ containing row vectors of shape functions evaluated at the contact points between the axles and the rail as well as the total reaction vector $\bar{\mathbf{f}}_{\mathrm{I}}^t$ between the train axles and the bridge.

4. FORMULATION OF TRAIN-BRIDGE SYSTEM

The vertical displacement $y(x, t)$ of an axle depends on the vertical displacement of the bridge $y_b(x, t)$ and the rail irregularity $r(x)$ at the same location, i.e.,

$$y(x, t) = y_b(x, t) + r(x), \tag{14}$$

in which x denotes the horizontal position of the axles. The vertical displacement of the bridge $y_b(x, t)$ at the contact point can be expressed in terms of the nodal displacement vector $\delta_b^e(t)$ of the beam element carrying the axle as

$$y_b(x, t) = \mathbf{N}_b^e(x)\delta_b^e(t), \tag{15}$$

where $\mathbf{N}_b^e(x)$ is the matrix containing the shape functions of the beam element. Combining equations (14) and (15) gives

$$y(x, t) = \mathbf{N}_b^e(x)\delta_b^e(t) + r(x). \tag{16}$$

The axles of the train may be straddling many elements at a time. Equation (16) can therefore be expanded to cover all axles, i.e.,

$$\delta_{\mathrm{I}}^t(\mathbf{x}, t) = \mathbf{N}_b(\mathbf{x})\delta_b(t) + \mathbf{r}(\mathbf{x}), \tag{17}$$

where $\mathbf{N}_b(\mathbf{x})$ is the shape function matrix evaluated at the contact points between the axles and the rail, $\delta_b(t)$ is the displacement vector of the bridge and $\mathbf{r}(\mathbf{x})$ is a vector containing the rail irregularities at the contact points. The vertical velocity vectors $\dot{\delta}_{\mathrm{I}}^t$ and the vertical acceleration $\ddot{\delta}_{\mathrm{I}}^t$ can therefore be obtained accordingly as

$$\dot{\delta}_{\mathrm{I}}^t = \mathbf{N}_b\dot{\delta}_b + v\mathbf{N}_b'\delta_b + v\mathbf{r}', \tag{18}$$

$$\ddot{\delta}_{\mathrm{I}}^t = \mathbf{N}_b\ddot{\delta}_b + 2v\mathbf{N}_b'\dot{\delta}_b + v^2\mathbf{N}_b''\delta_b + a\mathbf{N}_b'\delta_b + a\mathbf{r}' + v^2\mathbf{r}'' \tag{19}$$

in which v and a stand for the horizontal velocity and acceleration of the train, respectively, and the prime denotes the differentiation with respect to x, and the independent variables are omitted for simplicity. Substituting equations (17–19) into equation (8) and combining with equation (13), the equation of motion of the entire train–bridge system can be written as

$$\mathbf{m}\ddot{\delta} + \mathbf{c}\dot{\delta} + \mathbf{k}\delta = \mathbf{p}, \tag{20}$$

where $\mathbf{m}$, $\mathbf{c}$, $\mathbf{k}$, $\mathbf{p}$ and δ are the mass matrix, damping matrix, stiffness matrix, load vector and displacement vector for the entire train–bridge system respectively. Equation (20) can also be written in partitioned form as

$$\begin{bmatrix} \mathbf{m}_{uu}^t & \\ & \mathbf{m}_{bb} \end{bmatrix} \begin{Bmatrix} \ddot{\delta}_u^t \\ \ddot{\delta}_b \end{Bmatrix} + \begin{bmatrix} \mathbf{c}_{uu}^t & \mathbf{c}_{tb} \\ \mathbf{c}_{bt} & \mathbf{c}_{bb} \end{bmatrix} \begin{Bmatrix} \dot{\delta}_u^t \\ \dot{\delta}_b \end{Bmatrix} + \begin{bmatrix} \mathbf{k}_{uu}^t & \mathbf{k}_{tb} \\ \mathbf{k}_{bt} & \mathbf{k}_{bb} \end{bmatrix} \begin{Bmatrix} \delta_u^t \\ \delta_b \end{Bmatrix} = \begin{Bmatrix} \mathbf{p}_u^t \\ \mathbf{p}_b \end{Bmatrix}, \tag{21}$$

in which the sub-matrices and sub-vectors are given as

$$\mathbf{m}_{bb} = \mathbf{m}_b + \mathbf{N}_b^{\mathrm{T}}\mathbf{m}_{\mathrm{II}}^t\mathbf{N}_b, \quad \mathbf{c}_{tb} = \mathbf{c}_{u\mathrm{I}}^t\mathbf{N}_b, \tag{22, 23}$$

$$\mathbf{c}_{bt} = \mathbf{N}_b^{\mathrm{T}}\mathbf{c}_{\mathrm{I}u}^t, \quad \mathbf{c}_{bb} = \mathbf{c}_b + 2v\mathbf{N}_b^{\mathrm{T}}\mathbf{m}_{\mathrm{II}}^t\mathbf{N}_b' + \mathbf{N}_b^{\mathrm{T}}\mathbf{c}_{\mathrm{II}}^t\mathbf{N}_b, \tag{24, 25}$$

$$\mathbf{k}_{tb} = vc_{u\mathrm{I}}^t\mathbf{N}_b' + \mathbf{k}_{u\mathrm{I}}^t\mathbf{N}_b, \quad \mathbf{k}_{bt} = \mathbf{N}_b^{\mathrm{T}}\mathbf{k}_{\mathrm{I}u}^t, \tag{26, 27}$$

$$\mathbf{k}_{bb} = \mathbf{k}_b + v^2\mathbf{N}_b^{\mathrm{T}}\mathbf{m}_{\mathrm{II}}^t\mathbf{N}_b'' + a\mathbf{N}_b^{\mathrm{T}}\mathbf{m}_{\mathrm{II}}^t\mathbf{N}_b' + v\mathbf{N}_b^{\mathrm{T}}\mathbf{c}_{\mathrm{II}}^t\mathbf{N}_b' + \mathbf{N}_b^{\mathrm{T}}\mathbf{k}_{\mathrm{II}}^t\mathbf{N}_b, \tag{28}$$

$$\mathbf{p}_u^t = -(v\mathbf{c}_{u\mathrm{I}}^t\mathbf{r}' + \mathbf{k}_{u\mathrm{I}}^t\mathbf{r}), \quad \mathbf{p}_b = -\mathbf{N}_b^{\mathrm{T}}(\mathbf{R}_w + a\mathbf{m}_{\mathrm{II}}^t\mathbf{r}' + v^2\mathbf{m}_{\mathrm{II}}^t\mathbf{r}'' + v\mathbf{c}_{\mathrm{II}}^t\mathbf{r}' + \mathbf{k}_{\mathrm{II}}^t\mathbf{r}). \tag{29, 30}$$

The problem is then solved by direct integration using the Wilson θ method or similar methods [19]. However, the matrices and vectors in the equation of motion for the train–bridge system are time-dependent. In particular, the number of railway vehicles acting on the bridge and the positions of axles have to be checked so that the mass matrix $\mathbf{m}_t$, the damping matrix $\mathbf{c}_t$, the stiffness matrix $\mathbf{k}_t$ and the load vector $\mathbf{p}_t$ at time t are updated accordingly.

5. CASE STUDY

Figure 4 shows the simplified model of an actual cable-stayed bridge. The bridge is provided with four anchor piers, which include two end piers and two intermediate piers anchoring the middle of each side span. The cables have a semi-fan arrangement. The bridge is generally symmetrical except for the support arrangement. The bridge deck is hinged at Tower C but permitted to slide longitudinally on bearings installed on Tower D and all other piers. The cables are numbered sequentially starting from the leftmost cable. The relevant properties of the bridge and the finite element mesh are given in Table 1. The modulus of elasticity for the main span of the deck and all cables is taken as 200 GPa. The modulus of elasticity for the side spans of the each and the towers is taken as 35 GPa. A train comprising a locomotive and seven carriages is considered to cross the bridge at a speed ranging from 0 to 200 km/h. The basic data of the train model used are shown in Table 2. The rail irregularity is expressed is a sinusoidal manner as $r(x) = A_s \sin(2\pi x/L_s)$, in which the amplitude is taken as $A_s = 0{\cdot}005$ m and the wavelength is taken as $L_s = 11{\cdot}5$ m.

To assess the results, the impact factor is calculated as follows:

$$I = (R_d(x) - R_s(x))/R_s(x), \tag{31}$$

in which $R_d(x)$ and $R_s(x)$ are, respectively, the maximum dynamic and static responses of the bridge at the location x resulting from the passage of the train. Note that the maximum dynamic response $R_d(x)$ and the maximum static response $R_s(x)$ may be caused by the train at different locations. The response may be the displacement, bending moment or cable tension at the component concerned. Certain parts of the bridge have been selected for a detailed study of the impact effect. For the bridge deck, the cross-sections chosen include Section G (midway between Piers A and B), Section B (directly above Pier B), Section H (midway

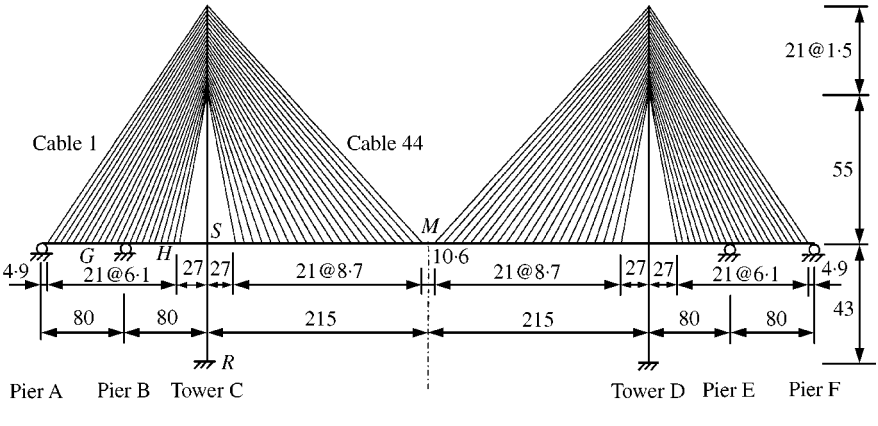

Figure 4. Simplified model of a cable-stayed bridge (dimensions in m).

TABLE 1

Properties of the cable-stayed bridge

Member	Number of elements	Cross-sectional area (m^2)	Moment of inertia (m^4)	Mass per unit length (ton/m)
Deck side spans AC and DF	24, 24	48.49	613·138	220·0
Deck main span CD	46	19·56	173·876	60·0
Towers C and D above deck (between anchorages)	21, 21	41·90	197·757	111·035
Towers C and D above deck (below anchorages)	2, 2	45·40	288·675	120·311
Towers C and D below deck	3, 3	88·62	1717·345	234·843
Cables 1–5 and 84–88	1 each	0·03195	—	0·250
Cables 6–11 and 78–83	1 each	0·02825	—	0·222
Cables 12–14 and 75–77	1 each	0·02456	—	0·193
Cables 15–17 and 72–74	1 each	0·02225	—	0·175
Cables 18–21 and 68–71	1 each	0·01763	—	0·138
Cables 22–23 and 66–67	1 each	0·02502	—	0·196
Cables 24–27 and 62–65	1 each	0·01670	—	0·131
Cables 28–30 and 59–61	1 each	0·01901	—	0·149
Cables 31–33 and 56–58	1 each	0·02363	—	0·185
Cables 34–39 and 50–55	1 each	0·02687	—	0·211
Cables 40–49	1 each	0·03010	—	0·236

TABLE 2

Basic data of the train model

Data	Locomotive	Carriage
Mass of vehicle body m_v(t)	90·958	34·0
Mass of each bogie frame m_f(t)	10·175	3·0
Mass of each axle together with wheels m_w(t)	4·522	1·4
Moment of inertia of vehicle body I_v(tm^2)	2880·0	2086·0
Moment of inertia of each bogie frame I_f(tm^2)	226·3	3·47
Stiffness of spring in secondary suspension k_1(kN/m)	55000	550
Stiffness of spring in primary suspension k_2(kN/m)	10710	1000
Distance between two centres of bogie frames l_1(m)	12·0	9·0
Distance between two centres of axles l_2(m)	3·6	2·4
Overall length of vehicle body l_3 (m)	23·1	26·575

between Pier B and Tower C), Section S (directly above Tower C) and Section M (midway between Tower C and Tower D), as shown in Figure 4. Section R at the base of the Tower C is chosen to study the effect on the base moment. Cables 1, 7, 22, 23, 33 and 44 are chosen to monitor the variation of cable tension. In the analysis, the interaction forces between the train and the bridge are being monitored to make sure that no separation has occurred [20].

5.1. EFFECT OF DAMPING

The damping characteristics of the bridge and the train vehicles are very important parameters influencing the dynamic response of a cable-stayed bridge. However, these

TABLE 3

Constants for Rayleigh damping of train vehicles and bridge

	Frequency f_1 (Hz)	Frequency f_2 (Hz)	Coefficient α	Coefficient β
Locomotive	2·76	4·21	0·0005	0·0025
Caarriage	0·85	1·38	0·0015	0·0075
Cable-stayed bridge	0·35	0·60	0·0040	0·0200

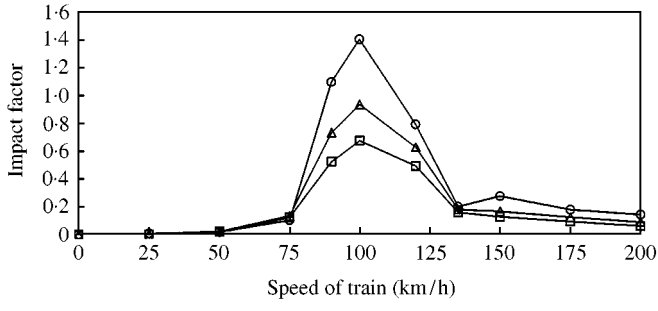

Figure 5. Impact factors based on bending moment at Section G of deck: —□—, damping case 1; —△—, damping case 2; —○—, damping case 3.

damping parameters are often difficult to assess with accuracy and the damping parameters for the chosen train are not available. Therefore, Rayleigh damping [19] has been adopted in the present study. For example, the damping matrix $\mathbf{c}_b$ of the bridge takes the form $\mathbf{c}_b = \alpha\mathbf{m}_b + \beta\mathbf{k}_b$ where α and β are constants determined from the two given or assumed damping ratios corresponding to the two lowest frequencies of vibration determined from the free vibration analysis using finite element method. The constants α and β for the train vehicles can be similarly obtained. The parameters adopted in the present study are shown in Table 3, which correspond to damping ratios ranging from 2 to 4%. In the present study, three cases of damping are considered and the entire train comprising a locomotive and seven carriages has been used. In Case 1, the parameters shown in Table 3 are adopted whereas in Case 2, half of the values shown in Table 3 are adopted. In Case 3, all damping constants are considered as zero.

The impact factors based on bending moment at Section G of the deck are plotted in Figure 5. Figures 6 and 7, respectively, present the impact factors based on bending moment at Section R of Tower C and those based on tension in Cable 22. The results for other sections are similar. The maximum impact factors and their associated speeds are extracted and presented in Table 4. It is observed that the maximum impact factors are mostly concentrated in the speed range of 90–100 km/h. One may be led to think that such pronounced impact effects are due to the excitation of the lower vibration modes caused by travelling on the sinusoidal rail irregularity. A simple check actually shows that the frequencies of such excitations are far from the lower natural frequencies of the bridge and the train vehicles. Figure 8 shows the impact factor based on the deflection at Section M of the deck. The low peaks at 100 km/h and the high-speed tail are unusual. However, as the impact factors in this case are generally very small, they cannot be taken as representative.

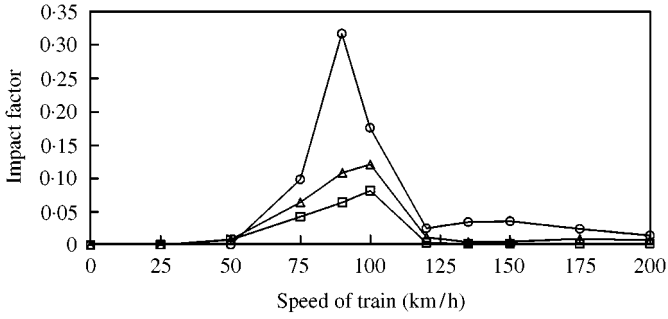

Figure 6. Impact factors based on bending moment at Section R of Tower C: —□—, damping case 1; —△—, damping case 2; —○—, damping case 3.

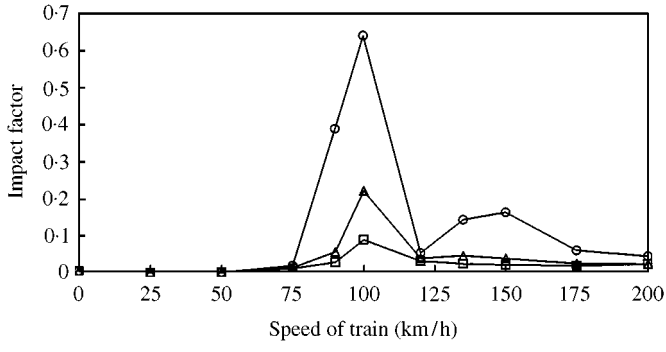

Figure 7. Impact factors based on tension in Cable 22. —□—, damping case 1; —△—, damping case 2; —○—, damping case 3.

TABLE 4

Effect of damping: maximum impact factors and associated speed

Load effects	Damping case 1		Damping case 2		Damping case 3	
	Impact factor	Speed (km/h)	Impact factor	Speed (km/h)	Impact factor	Speed (km/h)
Bending moment at Section B of deck	0·39	100	0·55	100	0·72	100
Bending moment at Section G of deck	0·67	100	0·93	100	1·40	100
Bending moment at Section H of deck	0·83	100	1·10	100	1·26	100
Bending moment at Section M of deck	0·06	100	0·09	100	0·12	100
Bending moment at Section S of deck	0·03	100	0·05	100	0·13	100
Bending moment at Section R of Tower C	0·08	100	0·12	100	0·32	90
Bending moment at Section S of Tower C	0·04	100	0·06	100	0·18	90
Tension in Cable 1	< 0·01	75	0·01	100	0·06	90
Tension in Cable 7	< 0·01	90	0·04	100	0·07	100
Tension in Cable 22	0·09	100	0·22	100	0·64	100
Tension in Cable 23	0·05	100	0·09	100	0·21	100
Tension in Cable 33	0·01	100	0·03	100	0·07	90
Tension in Cable 44	0·02	90	0·02	90	0·07	90

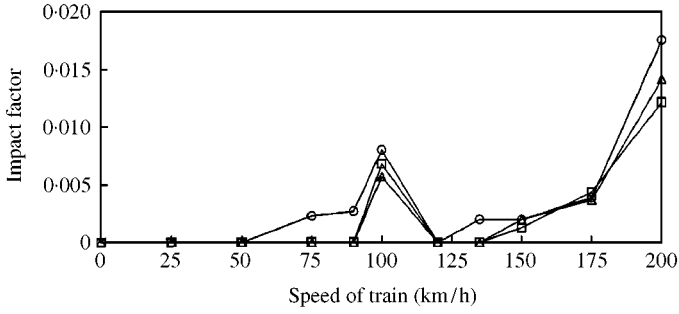

Figure 8. Impact factors based on deflection at Section M of deck: —□—, damping case 1; —△—, damping case 2; —○—, damping case 3.

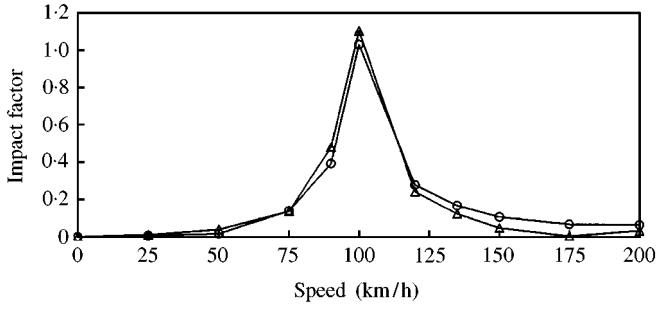

Figure 9. Comparison between a train and a solitary locomotive: impact factors based on bending moment at Section H of deck: —△—, train; —○—, solitary locomotive.

The impact effects based on the bending of deck are generally high at the side spans (i.e., sections G, B and H) but are much lower around the main span (i.e., Sections S and M). At the tower, the impact effects are moderate (i.e., Sections R and S). Very large variation in impact effects is observed among the cables. Most of the cables are subject to a very small impact effects. Exceptions are the short cables (e.g., Cables 22 and 23) which exhibit small to moderate impact effects. The impact effects based on deflection are normally close to zero, as shown in Figure 8 for Section M of the deck. Damping is generally effective to reduce the amount of impact.

5.2. EFFECT OF LENGTH OF TRAIN

The effect of the length of train on impact is then investigated. Two cases have been studied, and they are an entire train comprising a locomotive and seven carriages, and a solitary locomotive. When no damping is assumed (i.e., damping Case 3), separation between the train and the bridge is detected. Therefore, for the sake of comparison, damping Case 2, which does not give rise to any separation, has been chosen. Similar impact factors as in Section 5.1 have been calculated but only the representative ones are presented here. The impact factors based on bending moment at Section H of the deck are plotted in Figure 9. Figure 10 presents the impact factors based on bending moment at Section R of Tower C. The impact factors based on tension in Cables 23 are shown in Figure 11. Table 5 sums up the maximum impact factors and associated speeds. Figure 12 shows the impact factor based on deflection at Section M of the deck. It is observed that, with the

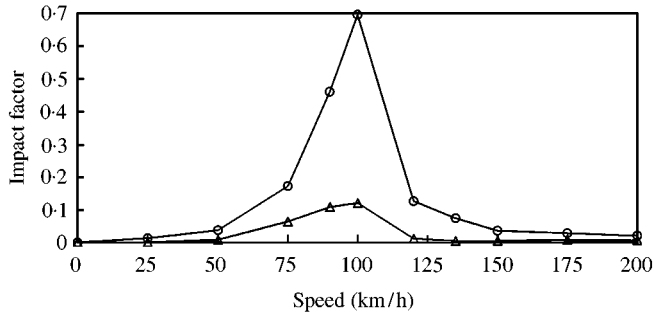

Figure 10. Comparison between a train and a solitary locomotive: impact factors based on bending moment at Section R of Tower C: —△—, train; —○—, solitary locomotive.

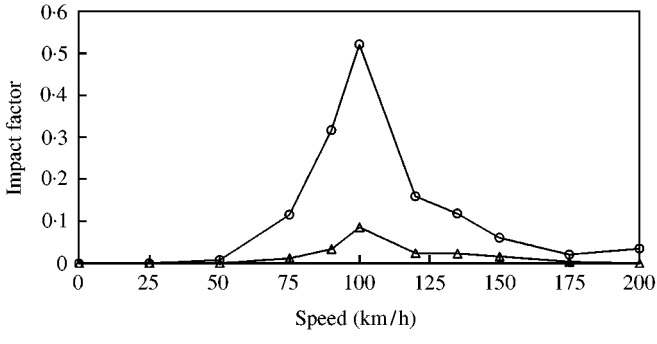

Figure 11. Comparison between a train and a solitary locomotive: impact factors based on tension in Cable 23: —△—, train; —○—, solitary locomotive.

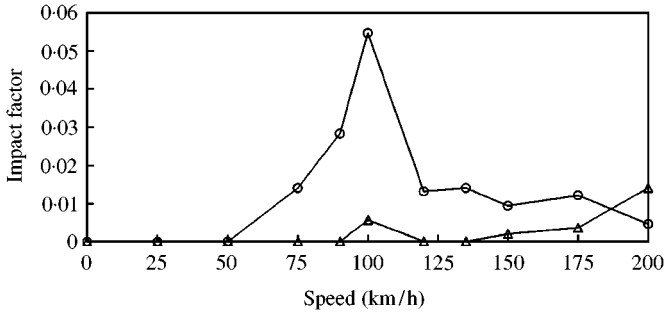

Figure 12. Comparison between a train and a solitary locomotive: impact factors based on deflection at Section M of deck: —△—, train; —○—, solitary locomotive.

exception of the impact factor based on bending at Section H of deck, the impact effects of a solitary locomotive are more significant than those of an entire train.

5.3. EFFECT OF TRAIN MODEL

As many different methods have been used to model the train vehicles, this section is devoted to the evaluation of their performance. The train model developed here can be

TABLE 5

Effect of length of train: maximum impact factors and associated speed

Load effects	Train		Solitary locomotive	
	Impact factor	Speed (km/h)	Impact factor	Speed (km/h)
Bending moment at Section H of deck	1·10	100	1·03	100
Bending moment at Section M of deck	0·09	100	1·15	100
Bending moment at Section S of deck	0·05	100	0·25	100
Bending moment at Section R of Tower C	0·12	100	0·69	100
Tension in Cable 23	0·09	100	0·52	100
Tension in Cable 33	0·03	100	0·22	100
Tension in Cable 44	0·02	90	0·08	90

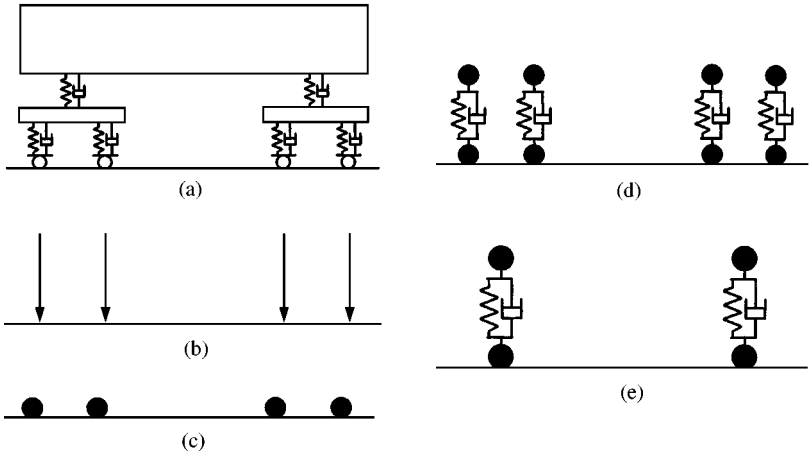

Figure 13. Models to represent a train vehicle: (a) train model; (b) 4-axle moving force model; (c) 4-axle moving mass model: (d) 4-axle 2-d.o.f. moving vehicle model; (e) 2-axle 2-d.o.f. moving vehicle model.

degenerated to various simplified models by setting certain components zero. Figure 13 shows the simplified models investigated. They include the train model, the 4-axle moving force model, the 4-axle moving mass model, the 4-axle 2-d.o.f. moving vehicle model, and the 2-axle 2-d.o.f. moving vehicle model. Damping Case 2 has been assumed. The mass, stiffness and damping of the train are assumed to be evenly distributed among various axles of the simplified model where applicable. Figures 14–16 show, respectively, the impact factors based on bending moments at Sections G and H of deck, and Section R of Tower C. The impact factors based on tension in Cable 22 are shown in Figure 17. Results from the train model can be regarded as the reference solutions. It is observed that the moving force and moving mass models far underestimate the impact effects. The model with 2 axles of 2-d.o.f. moving vehicles tends to overestimate the impact effects. The model with 4 axles of 2-d.o.f. moving vehicles tends to give fairly close prediction of impact effects. This is somehow expected, as it is closer to the train model with respect to the number of axles and suspension characteristics. The model with 4 axles of 2-d.o.f. moving vehicles is therefore a reasonable choice having due regard to accuracy and complexity of modelling.

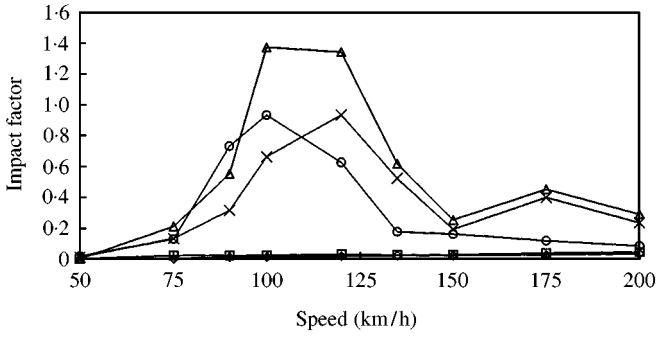

Figure 14. Comparison of various train models: impact factors based on bending moment at Section G of deck: —○—, train; —□—, 4-axle moving force; —◇—, 4-axle moving mass; —×—, 4-axle 2-d.o.f. vehicles; —△—, 2-axle 2-d.o.f. vehicles.

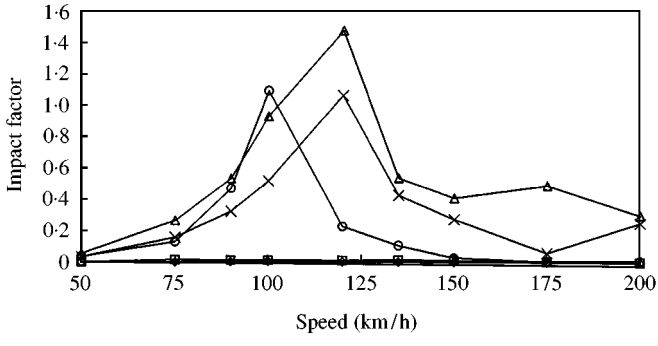

Figure 15. Comparison of various train models: impact factors based on bending moment at Section H of deck: —○—, train; —□—, 4-axle moving force; —◇—, 4-axle moving mass; —×—, 4-axle 2-d.o.f. vehicles; —△—, 2-axle 2-d.o.f. vehicles.

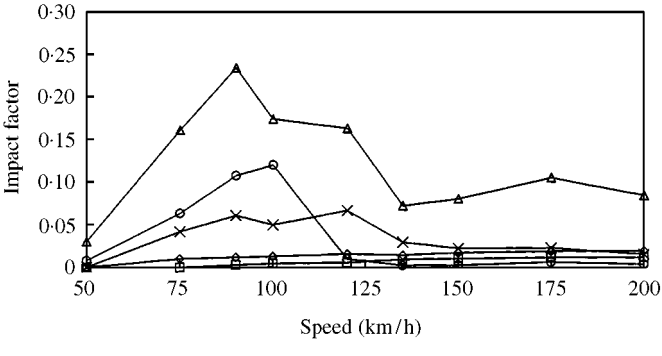

Figure 16. Comparison of various train models: impact factors based on bending moment at Section R of Tower C: —○—, train; —□—, 4-axle moving force; —◇—, 4-axle moving mass; —×—, 4-axle 2-d.o.f. vehicles; —△—, 2-axle 2-d.o.f. vehicles.

6. CONCLUSIONS

The impact effect of a moving train on a cable-stayed bridge is studied by modelling the bridge as a planar system and the train as a series of 4-axle vehicles. The rail irregularities and the geometric non-linear behaviour of the cable-stayed bridge are taken into account.

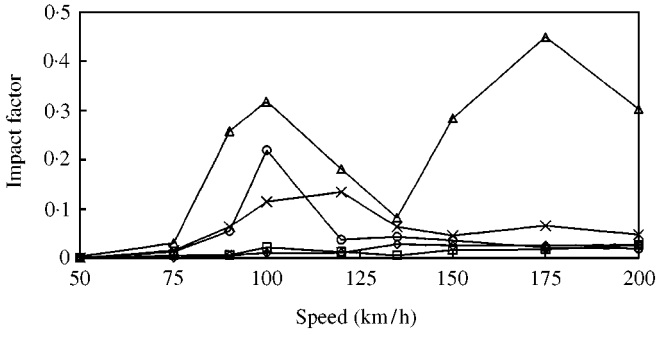

Figure 17. Comparison of various train models: impact factors based on tension in Cable 22: —○—, train; —□—, 4-axle moving force; —◇—, 4-axle moving mass; —×—, 4-axle 2-d.o.f. vehicles; —△—, 2-axle 2-d.o.f. vehicles.

The impact factors for various speeds are evaluated using a typical cable-stayed bridge and a sinusoidal irregularity profile. The influence of damping on impact factors is significant but it depends on the type of load effect considered and the location. The impact effect based on the bending of deck are generally high at the shorter side spans but are much lower around the much longer main span. At the tower, the impact effects are moderate. Very large variation in impact effects is observed among the cables. Most of the cables, with the exception of the shorter cables around the towers, are subject to very small impact effects. Damping is generally effective to reduce the amount of impact. The results show that the impact factor varies very much depending on the effect and the location studied, and such factors need to be adequately taken into account during the design.

The effect of the length of train on impact has also been investigated. It is observed that, in almost all cases, the impact effects of a solitary locomotive are more significant than those of an entire train. Various models for the train vehicle have been evaluated. It is observed that the moving force and moving mass models far underestimate the impact effects. The model with fewer axles of equivalent 2-d.o.f. moving vehicles tends to overestimate the impact effects while the model with the same number of axles of 2-d.o.f. moving vehicles tends to give fairly close prediction of impact effects.

ACKNOWLEDGMENTS

The financial support of the Hong Kong Research Grants Council is acknowledged. The authors are grateful to the reviewers for various useful suggestions.

REFERENCES

1. L. Fryba 1972 *Vibration of Solids and Structures Under Moving Loads*. Groningen, The Netherlands: Noordhoff International Publishing.
2. S. Timoshenko, D. H. Young and W. Weaver, Jr 1974 *Vibration Problems in Engineering*: 448–453. New York: John Wiley and Sons, fourth edition.
3. J. S. Wu and C. W. Dai 1987 *Journal of Structure Engineering, ASCE* **113**, 458–474. Dynamic responses of multispan nonuniform beam due to moving loads.
4. Y. B. Yang and J. D. Yau 1997 *Journal of Structural Engineering, ASCE* **123**, 1512–1518. Vehicle-bridge interaction for dynamic analysis.
5. F. H. Yang and G. A. Fonder 1998 *Journal of Engineering Mechanics, ASCE* **124**, 741–747. Dynamic response of cable-stayed bridge under moving loads.

6. D. Y. ZHENG, Y. K. CHEUNG, F. T. K. AU and Y. S. CHENG 1998 *Journal of Sound and Vibration* **212**, 455–467. Vibration of multi-span non-uniform beams under moving loads by using modified beam vibration functions.
7. M. OLSSON 1985 *Journal of Sound and Vibration* **99**, 1–12. Finite element, modal co-ordinate analysis of structures subjected to moving loads.
8. J. HINO, T. YOSHIMURA and N. ANANTHANARAYANA 1985 *Journal of Sound and Vibration* **100**, 477–491. Vibration analysis of non-linear beams subjected to a moving load using the finite element method.
9. Y. K. CHEUNG, F. T. K. AU, D. Y. ZHENG and Y. S. CHENG 1999 *Journal of Sound and Vibration* **228**, 611–628. Vibration of multi-span non-uniform bridges under moving vehicles and trains by using modified beam vibration functions.
10. A. S. VELETSOS and T. HUANG 1970 *Journal of Engineering Mechanics Division, ASCE* **96**, 593–620. Analysis of dynamic response of highway bridge.
11. O. COUSSY, M. SAID and J. P. VAN HOOVE 1989 *Journal of Sound and Vibration* **130**, 313–320. The influence of random surface irregularities on the dynamic response of bridges under suspended moving loads.
12. T. L. WANG and D. Z. HUANG 1992 *Journal of Structural Engineering, ASCE* **118**, 1354–1373. Cable-stayed bridge vibration due to road surface roughness.
13. T. H. T. CHAN and J. H. F. CHAN 1996 *Proceedings of Highways into the Next Century*, 24–26 *November* 1996, *Hong Kong*, 169–176. Parametric studies on highway bridge impact.
14. Y. B. YANG, J. D. YAU and L. C. HSU 1997 *Engineering Structures* **19**, 936–944. Vibration of simple beams due to trains moving at high speeds.
15. A WIRIYACHAI, K. H. CHU and V. K. GARG 1982 *Journal of Engineering Mechanics Division, ASCE* **108**, 648–655. Bridge impact due to wheel and track irregularities.
16. T. L. WANG, V. K. GARG and K. H. CHU 1991 *Journal of Structural Engineering, ASCE* **117**, 2099–2116. Railway bridge/vehicle interaction studies with new vehicle model.
17. Y. M. YANG, J. Y. PAN and Q. G. CHENG 1995 *China Railway Sciences, Beijing* **16**, 1–15. Theoretical and experimental studies of the dynamic response of long span railway bridges, in Chinese.
18. D. Z. HUANG and T. L. WANG 1992 *Computers & Structures* **43**, 897–908. Impact analysis of cable-stayed bridges.
19. K. J. BATHE and E. L. WILSON 1976 *Numerical Methods in Finite Element Analysis*. Englewood Cliffs, NJ: Prentice-Hall.
20. Y. K. CHEUNG, F. T. K. AU, Y. S. CHENG and D. Y. ZHENG 1999 *Journal of Sound and Vibration* **222**, 781–801. On the separation between moving vehicles and bridge.

APPENDIX A

The equations of motion of the vehicle body can be written as

$$m_v\ddot{y}_v + f_5 + f_6 = 0, \quad I_v\ddot{\theta}_v + (f_6 - f_5)l_1/2 = 0. \tag{A1, A2}$$

Similarly, the equations of motion of the bogie frames appear as

$$m_f\ddot{y}_{f1} + f_1 + f_2 - f_5 = 0, \quad I_f\ddot{\theta}_{f1} + (f_2 - f_1)l_2/2 = 0, \tag{A3, A4}$$

$$m_f\ddot{y}_{f2} + f_3 + f_4 - f_6 = 0, \quad I_f\ddot{\theta}_{f2} + (f_4 - f_3)l_2/2 = 0. \tag{A5, A6}$$

The equations of motion of the axles can be written as

$$m_w\ddot{y}_i - f_i - f_{ci} = 0 \quad \text{for } i = 1, 2, 3 \text{ and } 4 \tag{A7}$$

The dynamic reaction components f_1 to f_6 are dependent on the stiffnesses k_1 and k_2, and damping coefficients c_1 and c_2 of the suspension systems. The displacements y_5 to y_{10} can be related to the displacements at the centroid of the vehicle body y_v and θ_v, and the

displacements at the centroids of the bogie frames y_{f1}, θ_{f1}, y_{f2} and θ_{f2} as

$$y_5 = y_{f1} - \theta_{f1} l_2/2, \quad y_6 = y_{f1} + \theta_{f1} l_2/2, \tag{A8, A9}$$

$$y_7 = y_{f2} - \theta_{f2} l_2/2, \quad y_8 = y_{f2} + \theta_{f2} l_2/2, \tag{A10, A11}$$

$$y_9 = y_v - \theta_v l_1/2, \quad y_{10} = y_v + \theta_v l_1/2, \tag{A12, A13}$$

The dynamic reaction components f_1 to f_6 can therefore be written as

$$f_1 = k_2(y_{f1} - \theta_{f1} l_2/2 - y_1) + c_2(\dot{y}_{f1} - \dot{\theta}_{f1} l_2/2 - \dot{y}_1), \tag{A14}$$

$$f_2 = k_2(y_{f1} + \theta_{f1} l_2/2 - y_2) + c_2(\dot{y}_{f1} + \dot{\theta}_{f1} l_2/2 - \dot{y}_2), \tag{A15}$$

$$f_3 = k_2(y_{f2} - \theta_{f2} l_2/2 - y_3) + c_2(\dot{y}_{f2} - \dot{\theta}_{f2} l_2/2 - \dot{y}_3), \tag{A16}$$

$$f_4 = k_2(y_{f2} + \theta_{f2} l_2/2 - y_4) + c_2(\dot{y}_{f2} + \dot{\theta}_{f2} l_2/2 - \dot{y}_4), \tag{A17}$$

$$f_5 = k_1(y_v - \theta_v l_1/2 - y_{f1}) + c_1(\dot{y}_v - \dot{\theta}_v l_1/2 - \dot{y}_{f1}), \tag{A18}$$

$$f_6 = k_1(y_v + \theta_v l_1/2 - y_{f2}) + c_1(\dot{y}_v + \dot{\theta}_v l_1/2 - \dot{y}_{f2}), \tag{A19}$$

Substituting equations (A14–A19) into equations (A1–A7), the equations of motion of the train become

$$m_v \ddot{y}_v + 2c_1 \dot{y}_v - c_1(\dot{y}_{f1} + \dot{y}_{f2}) + 2k_1 y_v - k_1(y_{f1} + y_{f2}) = 0, \tag{A20}$$

$$I_v \ddot{\theta}_v + (c_1 l_1^2/2)\dot{\theta}_v + (c_1 l_1/2)(\dot{y}_{f1} - \dot{y}_{f2}) + (k_1 l_1^2/2)\theta_v + (k_1 l_1/2)(y_{f1} - y_{f2}) = 0, \tag{A21}$$

$$\begin{aligned} m_f \ddot{y}_{f1} - c_1 \dot{y}_v + (c_1 l_1/2)\dot{\theta}_v + (c_1 + 2c_2)\dot{y}_{f1} - c_2(\dot{y}_1 + \dot{y}_2) \\ - k_1 y_v + (k_1 l_1/2)\theta_v + (k_1 + 2k_2) y_{f1} - k_2(y_1 + y_2) = 0, \end{aligned} \tag{A22}$$

$$I_f \ddot{\theta}_{f1} + (c_2 l_2^2/2)\dot{\theta}_{f1} + (c_2 l_2/2)(\dot{y}_1 - \dot{y}_2) + (k_2 l_2^2/2)\theta_{f1} + (k_2 l_2/2)(y_1 - y_2) = 0, \tag{A23}$$

$$\begin{aligned} m_f \ddot{y}_{f2} - c_1 \dot{y}_v - (c_1 l_1/2)\dot{\theta}_v + (c_1 + 2c_2)\dot{y}_{f2} - c_2(\dot{y}_3 + \dot{y}_4) \\ - k_1 y_v - (k_1 l_1/2)\theta_v + (k_1 + 2k_2) y_{f2} - k_2(y_3 + y_4) = 0, \end{aligned} \tag{A24}$$

$$I_f \ddot{\theta}_{f2} + (c_2 l_2^2/2)\dot{\theta}_{f2} + (c_2 l_2/2)(\dot{y}_3 - \dot{y}_4) + (k_2 l_2^2/2)\theta_{f2} + (k_2 l_2/2)(y_3 - y_4) = 0, \tag{A25}$$

$$m_w \ddot{y}_1 - c_2 \dot{y}_{f1} + (c_2 l_2/2)\dot{\theta}_{f1} + c_2 \dot{y}_1 - k_2 y_{f1} + (k_2 l_2/2)\theta_{f1} + k_2 y_1 = f_{c1}, \tag{A26}$$

$$m_w \ddot{y}_2 - c_2 \dot{y}_{f1} - (c_2 l_2/2)\dot{\theta}_{f1} + c_2 \dot{y}_2 - k_2 y_{f1} + (k_2 l_2/2)\theta_{f1} + k_2 y_2 = f_{c2}, \tag{A27}$$

$$m_w \ddot{y}_3 - c_2 \dot{y}_{f2} + (c_2 l_2/2)\dot{\theta}_{f2} + c_2 \dot{y}_3 - k_2 y_{f2} + (k_2 l_2/2)\theta_{f2} + k_2 y_3 = f_{c3}, \tag{A28}$$

$$m_w \ddot{y}_4 - c_2 \dot{y}_{f2} - (c_2 l_2/2)\dot{\theta}_{f2} + c_2 \dot{y}_4 - k_2 y_{f2} - (k_2 l_2/2)\theta_{f2} + k_2 y_4 = f_{c4}, \tag{A29}$$

Equations (A20–A29) can be written in matrix notation in terms of the mass matrix $\mathbf{m}_t$, the damping matrix $\mathbf{c}_t$, the stiffness matrix $\mathbf{k}_t$ and the load vector $\mathbf{f}_t$ for the train vehicle as

$$\mathbf{m}_t \ddot{\delta}_t + \mathbf{c}_t \dot{\delta}_t + \mathbf{k}_t \delta_t = \mathbf{f}_t. \tag{A30}$$

The equation of motion for the train model can be written in terms of the sub-matrices and sub-vectors as

$$\begin{bmatrix} \mathbf{m}_{uu}^t & \\ & \mathbf{m}_{\mathrm{II}}^t \end{bmatrix} \begin{Bmatrix} \ddot{\delta}_u^t \\ \ddot{\delta}_{\mathrm{I}}^t \end{Bmatrix} + \begin{bmatrix} \mathbf{c}_{uu}^t & \mathbf{c}_{u\mathrm{I}}^t \\ \mathbf{c}_{\mathrm{I}u}^t & \mathbf{c}_{\mathrm{II}}^t \end{bmatrix} \begin{Bmatrix} \dot{\delta}_u^t \\ \dot{\delta}_{\mathrm{I}}^t \end{Bmatrix} + \begin{bmatrix} \mathbf{k}_{uu}^t & \mathbf{k}_{u\mathrm{I}}^t \\ \mathbf{k}_{\mathrm{I}u}^t & \mathbf{k}_{\mathrm{II}}^t \end{bmatrix} \begin{Bmatrix} \delta_u^t \\ \delta_{\mathrm{I}}^t \end{Bmatrix} + \begin{Bmatrix} \mathbf{f}_u^t \\ \mathbf{f}_{\mathrm{I}}^t \end{Bmatrix}, \tag{A31}$$

where the sub-matrices and sub-vectors are given below:

$$\mathbf{m}_{uu}^t = diag[m_v \;\; I_v \;\; m_f \;\; I_f \;\; m_f \;\; I_f], \tag{A32}$$

$$\mathbf{m}_{\mathrm{II}}^t = diag[m_w \;\; m_w \;\; m_w \;\; m_w], \tag{A33}$$

$$\mathbf{c}_{uu}^t = \begin{bmatrix} 2c_1 & 0 & -c_1 & 0 & -c_1 & 0 \\ 0 & c_1 l_1^2/2 & c_1 l_1/2 & 0 & -c_1 l_1/2 & 0 \\ -c_1 & c_1 l_1/2 & c_1 + 2c_2 & 0 & 0 & 0 \\ 0 & 0 & 0 & c_2 l_2^2/2 & 0 & 0 \\ -c_1 & -c_1 l_1/2 & 0 & 0 & c_1 + 2c_2 & 0 \\ 0 & 0 & 0 & 0 & 0 & c_2 l_2^2/2 \end{bmatrix}, \tag{A34}$$

$$\mathbf{c}_{u\mathrm{I}}^t = \begin{bmatrix} 0 & 0 & 0 & 0 \\ 0 & 0 & 0 & 0 \\ -c_2 & -c_2 & 0 & 0 \\ c_2 l_2/2 & -c_2 l_2/2 & 0 & 0 \\ 0 & 0 & -c_2 & -c_2 \\ 0 & 0 & c_2 l_2/2 & -c_2 l_2/2 \end{bmatrix} = (\mathbf{c}_{\mathrm{I}u}^t)^{\mathrm{T}}, \tag{A35}$$

$$\mathbf{c}_{\mathrm{II}}^t = diag[c_2 \;\; c_2 \;\; c_2 \;\; c_2], \tag{A36}$$

$$\mathbf{k}_{uu}^t = \begin{bmatrix} 2k_1 & 0 & -k_1 & 0 & -k_1 & 0 \\ 0 & k_1 l_1^2/2 & k_1 l_1/2 & 0 & -k_1 l_1/2 & 0 \\ -k_1 & k_1 l_1/2 & k_1 + 2k_2 & 0 & 0 & 0 \\ 0 & 0 & 0 & k_2 l_2^2/2 & 0 & 0 \\ -k_1 & -k_1 l_1/2 & 0 & 0 & k_1 + 2k_2 & 0 \\ 0 & 0 & 0 & 0 & 0 & k_2 l_2^2/2 \end{bmatrix}, \tag{A37}$$

$$\mathbf{k}_{u\mathrm{I}}^t = \begin{bmatrix} 0 & 0 & 0 & 0 \\ 0 & 0 & 0 & 0 \\ -k_2 & -k_2 & 0 & 0 \\ k_2 l_2/2 & -k_2 l_2/2 & 0 & 0 \\ 0 & 0 & -k_2 & -k_2 \\ 0 & 0 & k_2 l_2/2 & -k_2 l_2/2 \end{bmatrix} = (\mathbf{k}_{\mathrm{I}u}^t)^{\mathrm{T}}, \tag{A38}$$

$$\mathbf{k}_{\mathrm{II}}^{t} = diag[k_2 \;\; k_2 \;\; k_2 \;\; k_2], \tag{A39}$$

$$\mathbf{f}_{u}^{t} = [0 \;\; 0 \;\; 0 \;\; 0 \;\; 0 \;\; 0]^{\mathrm{T}}, \tag{A40}$$

$$\mathbf{f}_{\mathrm{I}}^{t} = [f_{c1} \;\; f_{c2} \;\; f_{c3} \;\; f_{c4}]^{\mathrm{T}}. \tag{A41}$$